

Superradiance as a witness to multipartite entanglement

Frederik Lohof,¹ Daniel Schumayer,² David A. W. Hutchinson,^{2,3} and Christopher Gies¹

¹*Institute for Theoretical Physics and Bremen Center for Computational Material Science,
University of Bremen, 28359 Bremen, Germany*

²*Dodd-Walls Centre, Department of Physics, University of Otago, Dunedin 9016, New Zealand*

³*Centre for Quantum Technologies, National University of Singapore, Singapore 117543*

(Dated: March 23, 2023)

Generation and detection of entanglement is at the forefront of most quantum information technologies. There is a plethora of techniques that reveal entanglement on the basis of only partial information about the underlying quantum state including, in particular, entanglement witnesses. Superradiance refers to the phenomenon of highly synchronized photon emission from an ensemble of quantum emitters that is caused by correlations among the individual particles and has been connected by Dicke himself to the presence of multipartite entangled states. We investigate this connection in a quantitative way and discuss, whether or not signatures of superradiance from semiconductor nanolasers, manifesting themselves as a modification of the spontaneous-emission time, can be interpreted as a witness to detect entanglement in the underlying state of the emitters.

Keywords: Quantum entanglement, superradiance, cavity QED, nanolasers

Radiative coupling between localized emitters has been of recurrent interest in different research areas over the past decades [1–6]. In a simple picture, coupling to a common light field can cause spatially distant emitters to align dipoles, resulting in correlated emission phenomena [7]. Well known effects that arise from this are sub- and superradiance – correlation-induced modifications of spontaneous emission due to the presence of other emitters that can enhance or reduce the spontaneous emission rate, respectively. While coupling via the free-space radiation field requires emitters to be close together [1] or regularly positioned [8] for the effect to occur, these conditions can be relaxed if emitters couple to a common mode of a microcavity. This situation has been investigated in the past, and signatures of sub- and superradiant emission have been demonstrated in ensembles of quantum dots [4, 9, 10], quantum wells [11], and superconducting circuits [12, 13]. Dicke described the phenomenon of sub- and superradiance in terms of collective states that are eigenstates equivalent to those of the total angular momentum. The maximal angular momentum states with $j = N/2$ are known today as Dicke states. They are multipartite entangled quantum states that can act as a resource for a range of different quantum information applications [14–16]. Dicke’s picture allows a somewhat different access to explaining the modification of spontaneous emission time in terms of dark and bright states [1, 17, 18]. Many consider the term superradiance to be bound to the emission from a Dicke state, whereas spontaneously created dipole correlations that also modify spontaneous emission in a similar manner are referred to as superfluorescence [19–21]. In a reciprocal way, it is not clear how far altered spontaneous emission behavior is indicative for the presence of Dicke states [22].

The purpose of this letter is to establish and quantify the connection between correlation-induced spontaneous emission-time modification and multi-partite entangle-

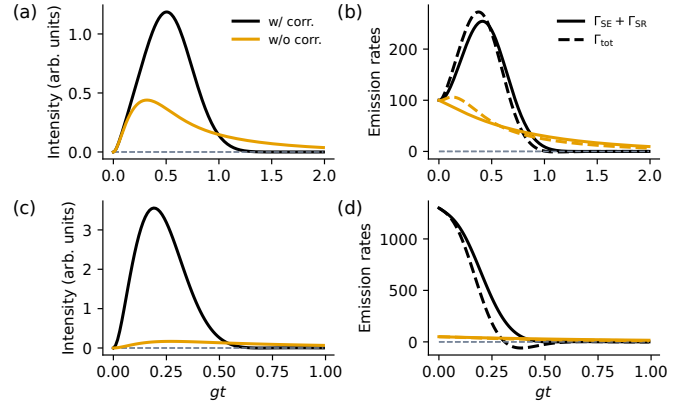


FIG. 1. (a) Comparison of emission from initially fully inverted emitters ($N = 50$) with (black) and without (orange) emitter correlations. (b) Combined spontaneous emission Γ_{SE} with superradiant enhancement Γ_{SR} (solid lines). Without emitter correlations $\Gamma_{SR} = 0$. Total emission Γ_{tot} (dashed) includes stimulated emission as well. (c)-(d) Same as above but with an emitter ensemble initially in a half inverted Dicke state $|D_{N,N/2}\rangle$. The half inverted Dicke state experiences the strongest emission enhancement. Parameters are $\gamma/g = 1$, $\kappa/g = 20$.

ment in terms of Dicke states. We consider quantum-dot based cavity-QED systems, but the interpretation and consequences apply to other systems as well. Determining entanglement in a multi-partite system is not trivial and no general measures apply. Here, we connect superfluorescent intensity bursts to entanglement witnesses for Dicke states that are related to electronic structure factors [23]. This is a particularly suitable approach, as this formulation of the entanglement witness directly relates to electronic correlation functions that are responsible for changes of the spontaneous emission time, and which are accessible by equation-of-motion techniques used in semiconductor quantum optics [7, 24, 25]. As we show, this

facilitates a natural connection between semiconductor quantum-optical methods and methods from quantum-information theory.

In the past, the presence of superradiant spontaneous emission enhancement has been seen as indicator for Dicke superradiance. Here, we present proof that in the superradiant regime, the emitter ensemble rarely transitions through an intermediate Dicke state with a high degree of entanglement, but instead a distinct interplay of sub- and superradiance is observed during light emission inhibiting the occurrence of detectable entanglement. We highlight how the occurrence of emitter correlations is a necessary but not sufficient condition for the presence of multipartite entanglement during the emission process.

Superradiant emission and entanglement. — Superradiance is caused by correlations between emitters and can arise in an ensemble of N emitters coupling to a common mode of an optical cavity. Dicke superradiance is associated with an increase of the spontaneous emission rate by a factor proportional to N^2 . To investigate this behavior, we use a model of N individual two-level emitters, such as atoms or semiconductor quantum dots, coupled to a single bosonic mode governed by the Tavis-Cummings Hamiltonian

$$H = \sum_i \frac{\omega_q}{2} \sigma_i^z + g \sum_i (\sigma_i^+ a + \sigma_i^- a^\dagger) + \omega_c a^\dagger a, \quad (1)$$

where ω_q and ω_c are the emitter and cavity resonance frequencies ($\hbar = 1$), and g is the light-matter interaction strength. The parafermionic operators σ_i^z and $\sigma_i^\pm = \frac{1}{2}(\sigma_i^x \pm i\sigma_i^y)$ are the emitter inversion, raising and lowering operators for emitter i [26], while a^\dagger and a are bosonic operators creating and annihilating photons in the cavity mode.

We consider an open quantum system [27] subject to emitter decay and photon losses at rates γ and κ , respectively. We apply the cluster expansion technique up to doublet level [24, 25] taking into account pair correlations between individual emitters. This well-established approach provides access to the dynamics of fundamental quantities, such as the output intensity, for large emitter ensembles in the weak coupling regime ($g^2/(\gamma + \kappa) \ll 1$). The temporal evolution of the photon number in the cavity $n(t)$ can be written as

$$\dot{n}(t) = \Gamma_{\text{SE}}(t) + \Gamma_{\text{StE}}(t) + \Gamma_{\text{CE}}(t) - \kappa n(t), \quad (2)$$

where the individual terms are the spontaneous emission (SE) rate $\Gamma_{\text{SE}} = cN(1 + \langle \sigma_z \rangle)$, stimulated emission (StE) $\Gamma_{\text{StE}} = cNn\langle \sigma_z \rangle$, and the correlated emission (CE), responsible for sub- and superradiant SE-time modifications $\Gamma_{\text{CE}} = 2cN(N-1)C_0$. Here, $C_0 = \langle \sigma_i^+ \sigma_j^- \rangle$ are emitter pair correlations. Importantly, the cluster expansion approach allows us to switch off and on these correlation contributions to assess their influence.

Fig. 1(a) shows the output intensity of an initially fully inverted system of $N = 50$ emitters with (black) and

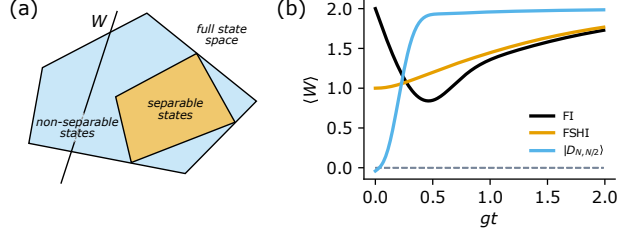


FIG. 2. (a) Schematic representation of the space of all physical states ρ with all separable states as a convex subset (orange). The witness W defines a hyperplane given by $\text{Tr}[W\rho] = 0$, bisecting the whole space into detected and non-detected states. (b) Structure factor witness $\langle W \rangle$ evaluated for different initial conditions: fully inverted (FI) emitters (black), fully-separable half-inverted (FSHI) product state (orange), and half-inverted Dicke state $|D_{N,N/2}\rangle$ (blue). Parameters are $N = 50$, $\kappa/g = 20$ and $\gamma/g = 1$.

without (orange) the influence of emitter correlations as a function of time. The well-known fingerprint associated with superfluorescence is apparent in the formation of an emission burst, during which most photons are emitted within a shortened time interval. Fig. 1(b) shows the corresponding emission rates. Without emitter correlations, the SE rate decays exponentially, while the presence of emitter correlations strongly enhances the emission rate before it falls beneath the uncorrelated value – these regimes are referred to as super- and subradiant. To verify that we truly are in a regime dominated by spontaneous emission, dashed lines show the total emission including stimulated contributions, which are small. In Fig. 1(c)-(d) we also show the emission output and emission rates from an ensemble with the same number of emitters that are initialized in the half-inverted Dicke state $|D_{N,N/2}\rangle$ at $t = 0$. Emission from this highly entangled state is strongly correlated and known to possess the largest emission-rate enhancement. It is eponymous for Dicke superradiance. The initial emission rates for Dicke states $|D_{N,k}\rangle$ are given by $\Gamma_{\text{CE}} = 2c(N-k)k = cN^2(1 - \langle \sigma_z \rangle^2)/4$, showing the proportionality to N^2 at a fixed inversion $\langle \sigma_z \rangle$. Without correlations, the spontaneous emission rate is $\Gamma_{\text{SE}} = c(2k - N) = cN\langle \sigma_z \rangle$ and only linear in N .

We now turn to the central question: to what extent is superradiant enhancement of spontaneous emission linked to the presence of entanglement between the correlated emitters? While for half-inverted Dicke state in Fig. 1(c),(d), entanglement is present by design, the situation is less clear for an initially fully inverted system (Fig. 1(a),(b)). As a tool, we employ an entanglement witness in the form of structure factors [23] given by

$$W = \mathbb{1} - \binom{N}{2}^{-1} \sum_{i < j} (c_x \sigma_i^x \sigma_j^x + c_y \sigma_i^y \sigma_j^y + c_z \sigma_i^z \sigma_j^z) \quad (3)$$

with real coefficients $|c_{x/y/z}| \leq 1$ and the binomial coefficient $\binom{n}{k}$. As shown in the schematic picture of Fig. 2(a),

the witness defines a hyperplane given by $\text{Tr}[W\rho] = 0$, dividing the space of all physical states into two parts, one ($\text{Tr}[W\rho] \geq 0$) containing the convex subset of all separable states (orange), and one ($\text{Tr}[W\rho] < 0$) containing all states that are said to be detected by the witness. Thus, a positive value for a witness is a necessary, but not a sufficient criterion for a state to be separable [28]. It has been shown that W for $c_x = c_y = 1$ and $c_z = -1$ detects states close to the half-inverted Dicke state $|D_{N,N/2}\rangle$ [23]. It is a key insight of this letter that in the context of our cluster-expansion formalism, this particular witness is directly connected to the correlated-emission term Γ_{CE} , which contains the same type to inter-emitter correlation. In fact, this connection has been one of the motivations for investigating the connection between entanglement and radiative-life time changes in the context of sub- and superradiance.

In the following we use techniques from the theory of permutationally invariant systems [29, 30], for which expectation values $\langle\sigma_i^\alpha\rangle$ and $\langle\sigma_i^\alpha\sigma_j^\alpha\rangle$ do not depend on the particle indices i, j . In this case, Eq. (3) reduces to

$$\langle W \rangle = 1 - 4\text{Re}[C_0] + C_{zz} \quad (4)$$

with $C_0 = \langle\sigma_i^+\sigma_j^-\rangle$ and $C_{zz} = \langle\sigma_i^z\sigma_j^z\rangle$ ($i \neq j$). Fig. 2(b) shows $\langle W \rangle$ for different initial conditions of an ensemble of 50 emitters. For initially fully inverted emitters (black curve), there is a significant dip in the witness expectation value during the emission that coincides with the maximal intensity output in Fig. 1(a). However, $\langle W \rangle$ stays far above the critical value of 0 required to signal the detection of entanglement. In the past, the initial burst of emission after excitation of the system was connected to the presence of Dicke states at the half-inversion point of the emission. Here, we show that Dicke states are *not* detected in this setup. Although it is hard to rule out entanglement in general, the large positive value of the witness shows a low overlap with Dicke states, from which we conclude that it is not merited to infer the presence of Dicke states from the superfluorescent emission burst. As a comparison, $\langle W \rangle$ is evaluated for a fully separable half-inverted product state (orange) $\rho_{\frac{1}{2}}^{\otimes N}$ with $\rho_{\frac{1}{2}} = \frac{1}{2}(|0\rangle\langle 0| + |1\rangle\langle 1|)$, and for the half-inverted Dicke state $\rho_{N,N/2} = |D_{N,N/2}\rangle\langle D_{N,N/2}|$. Both states have the same excitation level $\langle\sigma_z\rangle = 0$. While the separable state is not detected by W , the Dicke state is detected by construction of the witness and starts out with the minimal possible value of $\langle W \rangle = -2/(N-1)$ [23].

The fact that no entangled states close to Dicke states are detected during the emission highlights an important point of this work. While any build-up of emitter correlations causes an emission-rate modification that scales with N^2 , the mere presence of correlations is not a sufficient criterion to infer entanglement [22].

Pair correlations do not equal entanglement. —We investigate why, contrary to initial expectations, the emis-

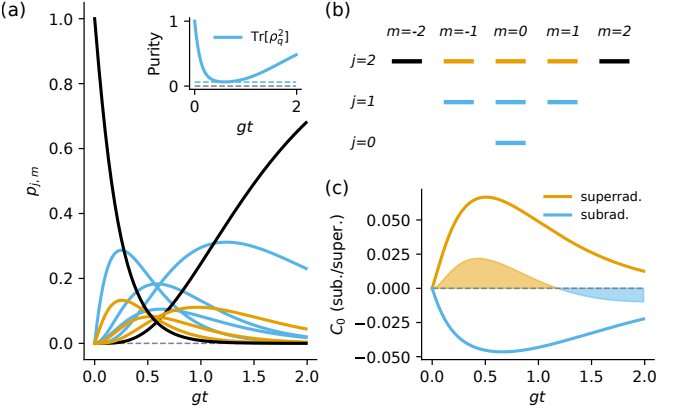


FIG. 3. (a) Decomposition of the reduced 4-emitter state into components $\rho_{j,m}$ according to Eq. (6). Colors indicate competing superradiant (orange), subradiant (blue) contributions as well as the separable ground and inverted state (black). In (b) the corresponding structure of possible angular momentum numbers (j, m) is shown. The inset shows the state purity $\text{Tr}[\rho_q^2]$ showing the transitive mixing of angular momentum components. Parameters are $N = 4$, $\kappa/g = 20$, $\gamma/g = 1$. (c) Emitter correlation C_0 separated by sub- and superradiant components, i.e. $C_0(j, m)$ from Eq. (9) weighted by the respective $p_{j,m}$. The shaded area indicates the sum of the two competing effects.

sion from an emitter ensemble does not necessarily involve the transitory creation of Dicke states and, thus, witnessing the corresponding entanglement. To do so, we analyze a system of fewer emitters that is amenable to a treatment by master equations for the system's density operator. We numerically integrate the Lindblad-von Neumann equation for an ensemble of 4 emitters. Given that we start with a permutationally invariant initial state, it can be shown [30] that the dynamics only couples permutationally invariant emitter states that are characterized by fixed (pseudo-) spin angular momentum eigenstates $|j, m\rangle$ of the collective spin operators \mathbf{J}^2 and J_z , where

$$J_\alpha = \frac{1}{2} \sum_i \sigma_i^\alpha, \quad \alpha \in \{x, y, z\}. \quad (5)$$

As a consequence we can decompose the marginal state of the emitters without the cavity sector as

$$\rho_q = \sum_j \sum_{m=-j}^j p_{j,m} \rho_{j,m}, \quad (6)$$

where (j, m) label the permutationally invariant components

$$\rho_{j,m} = \frac{1}{C_{jm}} \sum_{i=1}^{C_{jm}} |j, m, i\rangle\langle j, m, i| \quad (7)$$

with $\mathbf{J}^2 |j, m, i\rangle = j(j+1) |j, m, i\rangle$, $J_z |j, m, i\rangle = m |j, m, i\rangle$. The factor $C_{jm} = \frac{2j+1}{N+1} \binom{N+1}{\frac{N}{2}-j}$ is the multiplici-

ity of the irreducible representation (j, m) in the Clebsch-Gordan decomposition series for adding N (pseudo-) spin- $\frac{1}{2}$ systems. Note that $j_{\min} = 0$ ($\frac{1}{2}$) for even (odd) number of emitters, $j \leq \frac{N}{2}$ and $-j \leq m \leq j$.

In the following, we use the orthogonality relation

$$\text{Tr}[\rho_{j,m}\rho_{j',m'}] = \frac{1}{C_{jm}}\delta_{jj'}\delta_{mm'} \quad (8)$$

to extract the coefficients $p_{j,m}$ from any given ρ . In this notation, Dicke states are equivalent to the state with maximal $j = \frac{N}{2}$ with $|m| < j$, and have multiplicity $C_{jm} = 1$. Fig. 3(a) shows the contributions $p_{j,m}$ during the superradiant emission pulse. We see subsequent occupation of the entangled Dicke states during the evolution (orange), as well as large contributions from the separable, fully inverted state $|j, j\rangle$ and ground state $|j, -j\rangle$ (black). Furthermore, the dissipative processes in the Lindblad-von Neumann equation create contributions with lower total angular momentum $j < N/2$ (blue). Fig. 3(b) shows a diagram with all possible values of (j, m) .

Here, the main distinction between emission-rate modification and creation of entanglement is revealed. All permutationally invariant components $\rho_{j,m}$ of the emitter state (except for fully inverted and ground state) are non-separable, as can be shown by various entanglement measures such as the negativity (see the SI). However, the strong mixing of the entangled components leads to an overall separable state, as entanglement is strongly *sublinear* [28, 31]. The mixing is also reflected in the low purity $\text{Tr}[\rho_q^2]$ during the emission pulse shown in the inset of Fig. 3(a). In contrast, all emission-rate modifications considered here result from *linear* operator expectation values. This allows to analyze the emission rates in terms of linear combinations of the individual components with fixed (j, m) . The emitter correlations for any $\rho_{j,m}$ can be calculated explicitly and are given by (see the SI)

$$C_0(j, m) = \frac{j(j+1) - m^2 - \frac{N}{2}}{N(N-1)} \quad (9)$$

and

$$C_{zz}(j, m) = \frac{4m^2 - N}{N(N-1)}. \quad (10)$$

Fig. 3(c) shows the competition of sub- and superradiant contributions to the emission modification by separating all components $\rho_{j,m}$ according to their values of $C_0(j, m)$. The superradiant component is given by

$$C_0^{\text{super}} = \sum_{\substack{j, m \\ C_0(j, m) > 0}} p_{j,m} C_0(j, m), \quad (11)$$

and the subradiant one analogously. The colors in Fig. 3(b) are chosen to reflect the sub- or superradiant nature of the individual contributions. The shaded curve

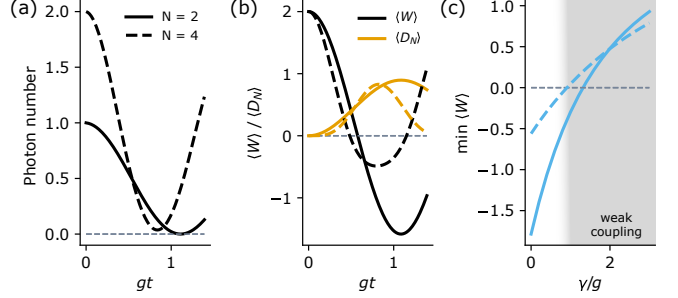


FIG. 4. Realization of Dicke states in the strong coupling regime for $N = 4$ (solid) and $N = 2$ (dashed) emitters. (a) Intracavity photon number starting from a well defined value $N/2$ $\kappa/g = 0.1$, $\gamma/g = 0.1$. (b) Structure factor witness $\langle W \rangle$ clearly showing detection of entangled states close to the half-inverted Dicke states as indicated by the expectation value $\langle D_N \rangle = \langle D_{N,N/2} | \rho_q | D_{N,N/2} \rangle$. (c) Minimum value for $\langle W \rangle$ as a function of emitter decay rate γ/g after initializing the system in the photon state as in (a), showing the limit of the coherent preparation of Dicke states.

in Fig. 3(c) shows the sum of the two contribution, i.e., the residual emitter correlation changing from a net superradiant to a subradiant behavior during the emission pulse. It is this residual emitter correlation that is the origin of the superfluorescent pulse observed in Figs. 1(a) and (b).

Coherent Dicke-state preparation. —Advances in quantum technology, and in particular cavity QED, make it possible to create well-defined photon states [32–34]. As we show, this opens the door for experiments that use Fock-state quantum light to generate entangled Dicke states in the dynamics of an emitter-cavity system. In Fig. 4 we show the dynamics of $N = 2$ (solid lines) and $N = 4$ (dashed) emitters strongly interacting with the cavity mode. As initial conditions, we assume Fock states of $n_p = \frac{N}{2}$ photons in the cavity. During the time evolution shown in Fig. 4(a), one clearly sees the detection of entanglement by the structure factor witness $\langle W \rangle$ (black lines Fig. 4(b)). Panel (b) further reveals the intermittent creation of the corresponding half-inverted Dicke state $|D_{N,N/2}\rangle$ (orange lines). The deterministic creation of the state $|D_{N,N/2}\rangle$ by the coherent dynamics can be explained in a simplified model that represents a generalization of the Jaynes-Cummings model to a multi-level emitter coupled to a cavity where the emitter levels are represented by the Dicke state $|N/2, m\rangle$. This is due to the fact that the Hamiltonian (1) commutes with the operator \mathbf{J}^2 and thus conserves the quantum number j .

The creation of Dicke-state entanglement in a deterministic fashion hinges on the ability to control the photon state in the cavity, and on the suppression of decoherence effects. To show this, we explicitly consider emitter dephasing over the range from strong to weak light-matter coupling and show the attainable entanglement in terms of the minimal value of $\langle W \rangle$ in Fig. 4(c). In the strong-

coupling regime, the system is truly found to be in an entangled state at the maximum of the first emission burst. With increasing dissipation rate γ , the overlap with the targeted Dicke state and the resulting entanglement reduces. At a single-emitter dissipation rate larger than $\gamma/g = 1.32$ (0.91) for $N = 2$ ($N = 4$) emitters, entanglement is no longer detected. As expected, the genuine multipartite entanglement becomes less robust to decoherence effects as the number of emitters increased.

Conclusion. —Dicke super- and subradiance is a recurrent topic in fundamental, atom- and semiconductor physics. Often it is viewed to be directly related to the modification of the spontaneous emission time in ensembles of correlated emitters. We have shown that contrary to this expectation, sub- and superradiance, as recently observed e.g., in nanolaser systems, is not linked to the existence of Dicke-states, but results from a mixture of (pseudo-) angular momentum eigenstates with both sub- and superradiant contributions that are mostly *not* Dicke-states. By combining methods from semiconductor optics and quantum information theory, we could establish a close connection between emitter correlations that modify the spontaneous emission rate, and a witness for detecting Dicke-state entanglement. We conclude that the famous emission pulse that is a recognized feature of Dicke superradiance is generally not indicative of entanglement, and in particular in recent demonstrations of superradiance in nanolasers, it is not caused by the emission from Dicke-states. Finally, we propose to use Fock-state quantum light to excite a cavity QED system, which can generate a transitory entangled Dicke state that can be discovered by an experimentally accessible entanglement witness. Then, the emission of superradiant light truly becomes a signature of multipartite entanglement within the emitter ensemble. We believe that this proposal has broad applicability and could lead to exciting new avenues of research in the field.

C. Gies is grateful for funding from the DAAD (Deutscher Akademischer Austauschdienst), facilitating a research sabbatical at the University of Otago and the Dodd Walls Centre. F. Lohof acknowledges funding from the central research development fund (CRDF) of the University of Bremen.

[1] R. H. Dicke, Coherence in Spontaneous Radiation Processes, *Physical Review* **93**, 99 (1954).

[2] J. H. Eberly, Superradiance Revisited, *American Journal of Physics* **40**, 1374 (1972).

[3] M. Gross and S. Haroche, Superradiance: An essay on the theory of collective spontaneous emission, *Physics Reports* **93**, 301 (1982).

[4] M. Scheibner, T. Schmidt, L. Worschech, A. Forchel, G. Bacher, T. Passow, and D. Hommel, Superradiance of quantum dots, *Nature Physics* **3**, 106 (2007).

[5] M. O. Scully and A. A. Svidzinsky, The Super of Superradiance, *Science* **325**, 1510 (2009).

[6] C. Hotter, L. Ostermann, and H. Ritsch, Cavity sub- and superradiance for transversely driven atomic ensembles, *Physical Review Research* **5**, 013056 (2023).

[7] H. A. M. Leymann, A. Foerster, F. Jahnke, J. Wiersig, and C. Gies, Sub- and Superradiance in Nanolasers, *Physical Review Applied* **4**, 044018 (2015).

[8] S. J. Masson and A. Asenjo-Garcia, Universality of Dicke superradiance in arrays of quantum emitters, *Nature Communications* **13**, 2285 (2022).

[9] F. Jahnke, C. Gies, M. Aßmann, M. Bayer, H. a. M. Leymann, A. Foerster, J. Wiersig, C. Schneider, M. Kamp, and S. Höfling, Giant photon bunching, superradiant pulse emission and excitation trapping in quantum-dot nanolasers, *Nature Communications* **7**, 11540 (2016).

[10] S. Kreinberg, W. W. Chow, J. Wolters, C. Schneider, C. Gies, F. Jahnke, S. Höfling, M. Kamp, and S. Reitzenstein, Emission from quantum-dot high- β microcavities: transition from spontaneous emission to lasing and the effects of superradiant emitter coupling, *Light: Science & Applications* **6**, e17030 (2017).

[11] G. Timothy Noe II, J.-H. Kim, J. Lee, Y. Wang, A. K. Wójcik, S. A. McGill, D. H. Reitze, A. A. Belyanin, and J. Kono, Giant superfluorescent bursts from a semiconductor magneto-plasma, *Nature Physics* **8**, 219 (2012).

[12] J. A. Mlynek, A. A. Abdumalikov, C. Eichler, and A. Wallraff, Observation of Dicke superradiance for two artificial atoms in a cavity with high decay rate, *Nature Communications* **5**, 5186 (2014).

[13] Z. Wang, H. Li, W. Feng, X. Song, C. Song, W. Liu, Q. Guo, X. Zhang, H. Dong, D. Zheng, H. Wang, and D.-W. Wang, Controllable Switching between Superradiant and Subradiant States in a 10-qubit Superconducting Circuit, *Physical Review Letters* **124**, 013601 (2020).

[14] R. Prevedel, G. Cronenberg, M. S. Tame, M. Paternostro, P. Walther, M. S. Kim, and A. Zeilinger, Experimental Realization of Dicke States of up to Six Qubits for Multipartite Quantum Networking, *Physical Review Letters* **103**, 020503 (2009).

[15] L. Pezzè, A. Smerzi, M. K. Oberthaler, R. Schmied, and P. Treutlein, Quantum metrology with nonclassical states of atomic ensembles, *Reviews of Modern Physics* **90**, 035005 (2018).

[16] J. Miguel-Ramiro and W. Dür, Delocalized information in quantum networks, *New Journal of Physics* **22**, 043011 (2020).

[17] V. V. Temnov and U. Woggon, Superradiance and Subradiance in an Inhomogeneously Broadened Ensemble of Two-Level Systems Coupled to a Low- Q Cavity, *Physical Review Letters* **95**, 243602 (2005).

[18] A. Auffèves, D. Gerace, S. Portolan, A. Drezet, and M. F. Santos, Few emitters in a cavity: from cooperative emission to individualization, *New Journal of Physics* **13**, 093020 (2011).

[19] R. Bonifacio and L. A. Lugiato, Cooperative radiation processes in two-level systems: Superfluorescence, *Physical Review A* **11**, 1507 (1975).

[20] Q. H. F. Vrehen, M. F. H. Schuurmans, and D. Polder, Superfluorescence: macroscopic quantum fluctuations in the time domain, *Nature* **285**, 70 (1980).

[21] K. Cong, Y. Wang, J.-H. Kim, G. T. Noe, S. A. McGill, A. Belyanin, and J. Kono, Superfluorescence from photoexcited semiconductor quantum wells: Magnetic field,

temperature, and excitation power dependence, *Physical Review B* **91**, 235448 (2015).

[22] G. Tóth, Detection of multipartite entanglement in the vicinity of symmetric Dicke states, *JOSA B* **24**, 275 (2007).

[23] P. Krammer, H. Kampermann, D. Bruß, R. A. Bertlmann, L. C. Kwek, and C. Macchiavello, Multipartite Entanglement Detection via Structure Factors, *Physical Review Letters* **103**, 100502 (2009).

[24] M. Kira and S. W. Koch, *Semiconductor Quantum Optics* (Cambridge University Press, Cambridge, 2011).

[25] C. Gies, J. Wiersig, M. Lorke, and F. Jahnke, Semiconductor model for quantum-dot-based microcavity lasers, *Physical Review A* **75**, 013803 (2007).

[26] L.-A. Wu and D. A. Lidar, Qubits as parafermions, *Journal of Mathematical Physics* **43**, 4506 (2002).

[27] H.-P. Breuer and F. Petruccione, *The Theory of Open Quantum Systems* (Oxford University Press, Oxford, New York, 2007).

[28] O. Gühne and G. Tóth, Entanglement detection, *Physics Reports* **474**, 1 (2009).

[29] M. Xu, D. A. Tieri, and M. J. Holland, Simulating open quantum systems by applying SU(4) to quantum master equations, *Physical Review A* **87**, 062101 (2013).

[30] N. Shammah, S. Ahmed, N. Lambert, S. De Liberato, and F. Nori, Open quantum systems with local and collective incoherent processes: Efficient numerical simulations using permutational invariance, *Physical Review A* **98**, 063815 (2018).

[31] A. O. Pittenger and M. H. Rubin, Convexity and the separability problem of quantum mechanical density matrices, *Linear Algebra and its Applications* **346**, 47 (2002).

[32] P. Bertet, S. Osnaghi, P. Milman, A. Auffeves, P. Maioli, M. Brune, J. M. Raimond, and S. Haroche, Generating and Probing a Two-Photon Fock State with a Single Atom in a Cavity, *Physical Review Letters* **88**, 143601 (2002).

[33] M. Hofheinz, E. M. Weig, M. Ansmann, R. C. Bialczak, E. Lucero, M. Neeley, A. D. O’Connell, H. Wang, J. M. Martinis, and A. N. Cleland, Generation of Fock states in a superconducting quantum circuit, *Nature* **454**, 310 (2008).

[34] M. Cooper, L. J. Wright, C. Söller, and B. J. Smith, Experimental generation of multi-photon Fock states, *Optics Express* **21**, 5309 (2013).